

# Unitarization effects in EFT predictions of VBS @LHC

Roberto A. Morales (work with C. García-García, M.J. Herrero)



Instituto de  
Física  
Teórica  
UAM-CSIC



Universidad Autónoma  
de Madrid

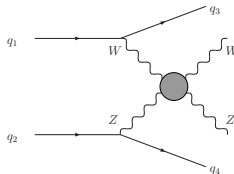
COMPOSE-IT: Unitarity for composite models and beyond in the HL-LHC era

Dipartimento di Fisica e Geologia (Università degli Studi di Perugia), 27-28 January 2020

Based on Phys. Rev. **D100** (2019) 096003 [1907.06668]

$$pp \rightarrow WZj_1j_2$$

by  $WZ \rightarrow WZ$  scattering



- Introduction: linear vs. non-linear EFT's
- The Electroweak Chiral Lagrangian (EChL)
- Aspects and implications of unitarity violation
- Restoring unitarity in  $WZ$  scattering at the LHC
- Parameter determination uncertainties
- Conclusions

# The (EW) Chiral symmetry in the SM and BSM

The Spontaneously Breaking Sector (SBS) of the SM can be written as

$$\mathcal{L}_{SBS} = \frac{1}{4} \langle \partial_\mu M^\dagger \partial^\mu M \rangle - \frac{\lambda}{4} \left( \frac{1}{2} \langle M^\dagger M \rangle + \frac{\mu^2}{\lambda} \right)^2$$

where  $M = \sqrt{2} \begin{pmatrix} \phi_0^* & \phi^+ \\ -\phi^- & \phi_0 \end{pmatrix}$  and the  $\Phi$  doublet is  $\begin{pmatrix} \phi^+ \\ \phi_0 \end{pmatrix}$ .

$\Rightarrow$  the  $\mathcal{L}_{SBS}$  is manifestly invariant under the global transformation:

$$M \rightarrow M' = g_L M g_R^\dagger \quad \text{with } g_L \in SU(2)_L \text{ and } g_R \in SU(2)_R$$

This global  $SU(2)_L \times SU(2)_R$  is called the EW Chiral symmetry.

It is spontaneously broken down to the diagonal subgroup

$$SU(2)_L \times SU(2)_R \rightarrow SU(2)_{L+R} \equiv SU(2)_{\text{Custodial}}$$

Gauge interactions ( $g' \neq 0$ ) and different fermion masses (in the same doublet) **explicitly break** the Chiral and Custodial symmetries.

**Main implication** of Custodial symmetry:  $\rho$  parameter value is close to 1!

# Linear approach to BSM: SMEFT

- The Higgs and the Goldstone bosons (GBs) form a left  $SU(2)$  doublet. In particular, the Higgs always appears in the combination  $H + v$ .
- The GBs **transform linearly** under the **Chiral symmetry**.
- Based on a **cutoff  $\Lambda$  expansion** (canonical dimension):

$$\mathcal{L}_{SMEFT} = \mathcal{L}_{SM} + \sum_i \frac{f_i^{(6)}}{\Lambda^2} \hat{\mathcal{O}}_i^{d=6} + \sum_i \frac{f_i^{(8)}}{\Lambda^4} \hat{\mathcal{O}}_i^{d=8} + \dots$$

- SMEFT typically emerges from **weakly interacting** UV theory.
- Typical situation when  $H$  is a fundamental field.

# Our approach to BSM: the non-linear EChL or HEFT

- The Goldstone bosons  $\pi^a$  are independent from the Higgs boson. In particular, the Higgs is a  $SU(2)$  singlet.
- The  $\pi^a$  **transform non-linearly** under the **Chiral symmetry**.
- Based on a **derivative expansion**  $\leftrightarrow$  Chiral expansion (powers of  $p$ ). Derivates and masses are soft scales of the EFT with power counting  $\mathcal{O}(p) \Rightarrow$  the  $\mathcal{L}$  is organized in terms of operators  $\mathcal{O}(p^2)$ ,  $\mathcal{O}(p^4)$ , ...
- Associated to **strongly interacting** UV theory.  
Natural scenario to generate dynamically resonances.
- Appropriate for composite models of the EWSB ( $H$  as a pseudo GB).
- **Non-trivial relation between linear and non-linear representations!**  
Some higher order operators, that were dim-8 in the linear representation, can contribute to a lower order in the non-linear one (dim-4 in the Chiral expansion).

# The Electroweak Chiral Lagrangian (EChL)

- Symmetries are Lorentz,  $CP$ , EW gauge  $SU(2)_L \times U(1)_Y$  and **Chiral**  $SU(2)_L \times SU(2)_R \rightarrow SU(2)_{L+R}$ . Based on ChPT of QCD.
- Light degrees of freedom and building blocks are:

Higgs boson as a singlet  $\Rightarrow \mathcal{F}(H) = 1 + 2a\frac{H}{v} + b\left(\frac{H}{v}\right)^2 + \dots$

EW gauge bosons  $\Rightarrow \hat{W}_\mu = gW_\mu^a \tau^a/2$ ,  $\hat{B}_\mu = g' B_\mu \tau^3/2$ ,  $\hat{W}_{\mu\nu}$ ,  $\hat{B}_{\mu\nu}$ .

EW GBs in  $U = \exp\left(\frac{i\pi^a \tau^a}{v}\right)$  that transforms linearly  $U \rightarrow g_L U g_R^\dagger$   
 $\Rightarrow D_\mu U = \partial_\mu U + i\hat{W}_\mu U - iU\hat{B}_\mu$  and  $\mathcal{V}_\mu = (D_\mu U)U^\dagger$ .

**Our assumptions:** fermion ints as in SM. Custodial sym preserved.

$$\mathcal{L}_{EChL} = \mathcal{L}_2 + \mathcal{L}_4 \text{ (relevant for VBS)}$$

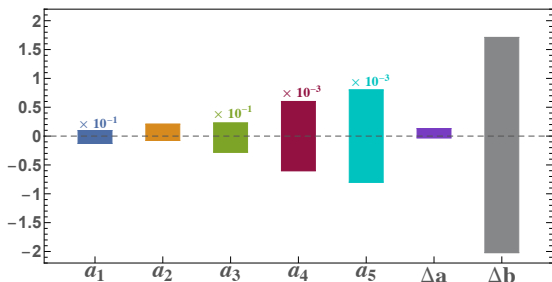
$$\begin{aligned} \mathcal{L}_2 = & -\frac{1}{2g'} \langle \hat{B}_{\mu\nu} \hat{B}^{\mu\nu} \rangle - \frac{1}{2g} \langle \hat{W}_{\mu\nu} \hat{W}^{\mu\nu} \rangle + \frac{1}{2} \partial_\mu H \partial^\mu H - V(H) \\ & + \frac{v^2}{4} \mathcal{F}(H) \langle D_\mu U^\dagger D^\mu U \rangle \end{aligned}$$

$$\begin{aligned} \mathcal{L}_4 = & a_1 \langle U \hat{B}_{\mu\nu} U^\dagger \hat{W}^{\mu\nu} \rangle + i a_2 \langle U \hat{B}_{\mu\nu} U^\dagger [\mathcal{V}^\mu, \mathcal{V}^\nu] \rangle - i a_3 \langle \hat{W}_{\mu\nu} [\mathcal{V}^\mu, \mathcal{V}^\nu] \rangle \\ & + a_4 \langle \mathcal{V}_\mu \mathcal{V}_\nu \rangle \langle \mathcal{V}^\mu \mathcal{V}^\nu \rangle + a_5 \langle \mathcal{V}_\mu \mathcal{V}^\mu \rangle \langle \mathcal{V}_\nu \mathcal{V}^\nu \rangle \end{aligned}$$

# EChL parameters and interactions



- SM predictions recovered for  $\Delta a = a - 1 = 0$ ,  $\Delta b = b - 1 = 0$  and  $a_i = 0$ .
- Only  $a$ ,  $b$ ,  $a_4$  and  $a_5$  survive *switching off* gauge interactions (limit  $g, g' \rightarrow 0$ ).  
Relevant parameters applying *Equivalence Theorem (ET)*:  
 $A(V_L V_L \rightarrow V_L V_L) \simeq A(\pi\pi \rightarrow \pi\pi)$



- Exp. bounds derived from  
[Pyhs. Rev. **D98** (2018) 030001 (PDG)  
Pyhs. Rev. **D99** (2019) 033001 (ATLAS)  
Phys. Lett. B **798** (2019) 134985 (CMS)  
Phys. Rev. **D101** 012002 (ATLAS)  
ATLAS-CONF-2019-030 (2001.05178)]

# Implications of unitarity violation in VBS

- VBS is a powerful observable to look for New Physics: extremely sensitive to SM deviations introduced by EChL operators. Quasi-direct access to Goldstone dynamics through the longitudinal components (Equivalence Theorem).
- In the EChL context, interactions among gauge bosons scale with the external momenta  $\Rightarrow$  pathological predictions when energy increases  $\Rightarrow$  **violation of unitarity of the  $S$  matrix!**
- Unitarity requires on each  $J^{th}$  partial wave of  $A(V_{\lambda_1} V_{\lambda_2} \rightarrow V_{\lambda_3} V_{\lambda_4})$

$$\text{Im}[a_{\lambda_1 \lambda_2 \lambda_3 \lambda_4}^J(s)] = \sum_{\lambda_a, \lambda_b} [a_{\lambda_1 \lambda_2 \lambda_a \lambda_b}^J(s)] [a_{\lambda_a \lambda_b \lambda_3 \lambda_4}^J(s)]^*$$

It is a **coupled system** among all helicity states!

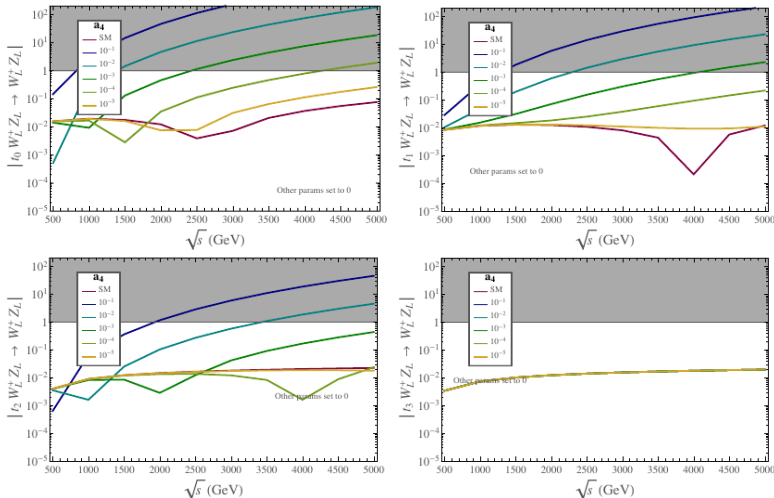
- Unitarity condition can be rewritten as  $|a^J(s)| \leq 1$  and defines the unitary violation energy scale. This scale depends on EChL parameters.
- As in the ChPT, unitarity condition is fulfilled perturbatively

$$\text{Im}[a_{\mathcal{O}(p^4)}^J(s)] = |a_{\mathcal{O}(p^2)}^J(s)|^2$$



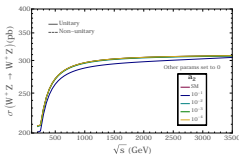
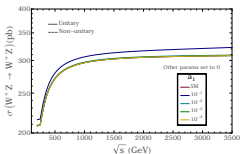
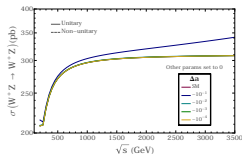
# Unitarity violation in $WZ$ scattering at partial wave level

As an example, consider the helicity state  $LL \rightarrow LL$  and study the effect of  $a_4$  in the partial wave amplitudes  $t_J$  corresponding to  $J = 0, 1, 2, 3$ .

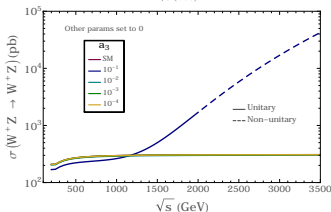


Next, consider the total cross section  $\sigma(W^+Z \rightarrow W^+Z)$

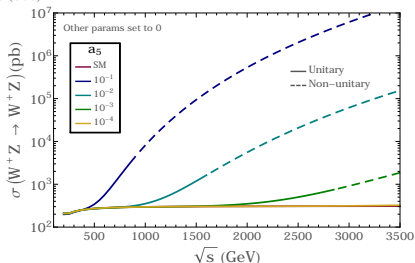
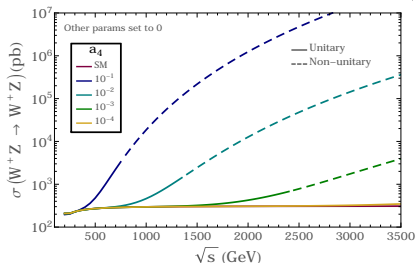
# Unitarity violation in $WZ$ scattering at subprocess level



$a_4$  and  $a_5$  are the most relevant parameters to unitarity violation!



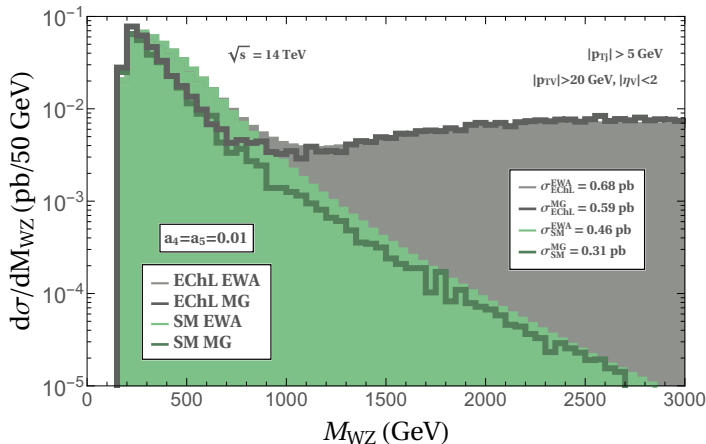
$a_{LLLL}^{J=0}(s)$  is the dominant contribution to unitarity violation!



# Unitarity violation in $WZ$ scattering at the LHC

Extrapolating this prediction at subprocess level in the prediction at the LHC process  $pp \rightarrow WZ + jj$

For example in the differential cross section: what happens above 1.5 TeV?



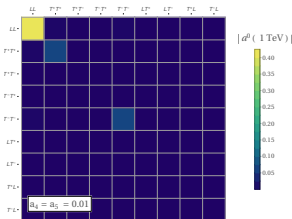
⇒ **unitarization for realistic predictions is mandatory!**

# Coupled helicities system

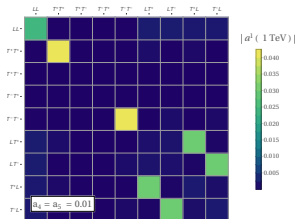
Looking at the partial wave amplitudes in order to fulfil unitarity condition:

- All the helicities channels ( $9 \times 9 = 81$ ) have to be considered consistently.

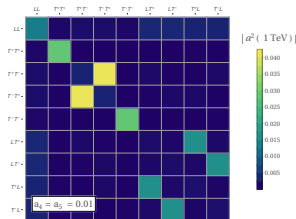
$J = 0$



$J = 1$



$J = 2$



- The  $i^{th}$  helicity amplitude grows with the CM energy like  $A_i \sim s^{\xi_i}$   
 $\Rightarrow$  eventually reach the unitarity limit  $|a_i^J| = 1$  at some scale  $s = \Lambda_i$ .
- Longitudinal modes only dominant for some  $J$ 's or  $(a_4, a_5)$  values.  
 In particular,  $\xi_{LLLL} = 2$  can be understood through the ET.

# Unitarization methods applied to the total amplitude

In order to provide unitary amplitude  $\hat{A}$ , several methods are implemented.

If we suppress *by hand* the pathological behaviour in the total amplitude:

- **Cut-Off**: limit the validity range of the EFT up to the minimal unitarity violation scale  $\Lambda$

$$\hat{A}(WZ \rightarrow WZ) = A(WZ \rightarrow WZ) \quad \text{for } s \leq \Lambda^2$$

- **Form Factor (FF)**: suppress the pathological behaviour via multiplying the amplitude by a smooth, continuous function

$$\hat{A}(WZ \rightarrow WZ) = A(WZ \rightarrow WZ) f^{\text{FF}} \quad \text{with } f^{\text{FF}} = (1 + s/\Lambda^2)^{-\xi}$$

- **Kink**: now the suppression is not smooth, but through a step function

$$f^{\text{Kink}} = \begin{cases} 1 & \text{if } s \leq \Lambda^2 \\ (s/\Lambda^2)^{-\xi} & \text{if } s > \Lambda^2 \end{cases}$$

# Unitarization methods applied to the partial waves

In the other two methods, unitarity is recovered from partial waves directly.

**Our proposal:**

$$\hat{A}_{\lambda_1 \lambda_2 \lambda_3 \lambda_4}(s, \cos \theta) = A_{\lambda_1 \lambda_2 \lambda_3 \lambda_4}(s, \cos \theta) + 16\pi \sum_{J=0}^2 (2J+1) d_{\lambda, \lambda'}^J(\cos \theta) \left( \hat{a}_{[\lambda_1 \lambda_2 \lambda_3 \lambda_4]}^J(s) - a_{\lambda_1 \lambda_2 \lambda_3 \lambda_4}^J(s) \right)$$

- **K-matrix:** an imaginary part is added such that the unitarity limit is saturated. The  $9 \times 9$  matrix **a** containing the whole coupled helicity system is reconstructed as

$$\hat{\mathbf{a}}^J = \mathbf{a}^J \cdot [\mathbf{1} - i \mathbf{a}^J]^{-1}$$

- **Inverse Amplitude Method (IAM):** from the contributions of  $\mathcal{O}(p^2)$  and  $\mathcal{O}(p^4)$  in the chiral expansion, the partial wave matrix amplitude is reconstructed as

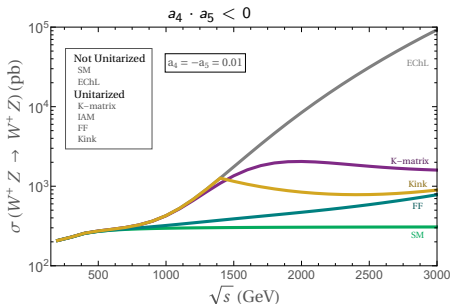
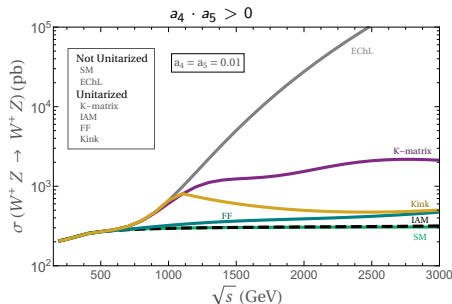
$$\hat{\mathbf{a}}^J = \mathbf{a}^{(2)J} \cdot [\mathbf{a}^{(2)J} - \mathbf{a}^{(4)J}]^{-1} \cdot \mathbf{a}^{(2)J}$$

A priori, no preferred unitarization method, but in this case:

Not only unitary predictions arise, but also the appropriate analytical structure  $\Rightarrow$  dynamically generated resonances can be accommodated with this procedure (as in ChPT for pion-pion scattering).

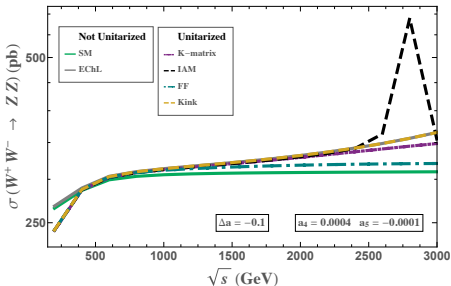
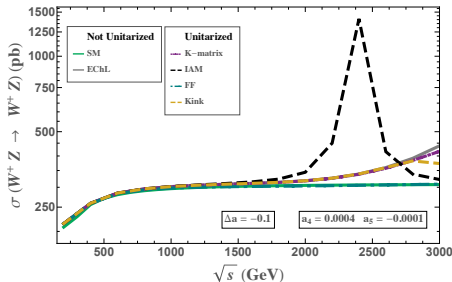
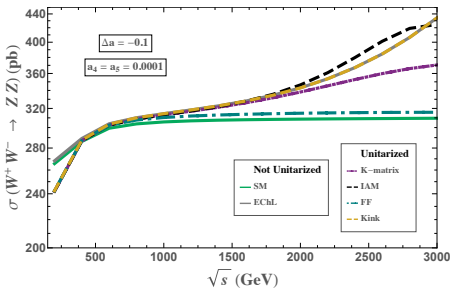
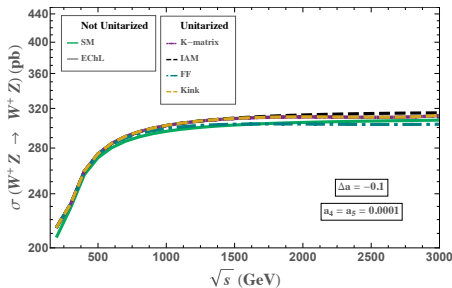
# Implications of unitarity at subprocess level

Applying the unitarization procedures to the  $WZ \rightarrow WZ$  total cross section  
**Very different predictions using different methods!**  $\Rightarrow$  the experimental constraints interpreted using one method or another will be different.



Then our aim is to give an estimate of the **theoretical uncertainty** in the experimental determination of  $a_4$  and  $a_5$  due to the unitarization scheme choice.

# More benchmark points: dynamical resonances in the IAM



We work here with non-resonant scenarios below  $4\pi v \sim 3$  TeV.



# Present experimental constraints: no consensus yet

Current bounds are given using one method at a time or no method at all.

- Some ATLAS analyses:

[Phys. Rev. D95 (2017) 032001]

use **K-matrix**

for  $a_{4(5)} = \alpha_{4(5)}$

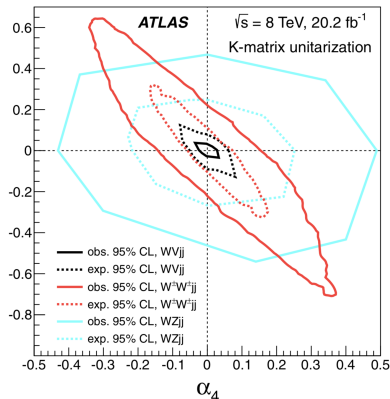
light blue contour at 95% C.L.

Our work focused in this Run 1

aQGC in VBS with final state  
 $W(l\nu)V(qq') + jj$

- Other ATLAS and CMS analyses:  
no unitarization method applied

$$a_{4(5)} = \frac{v^4}{16} \frac{f_{S0(S1)}}{\Lambda^4}$$



	Expected (WV) ( $\text{TeV}^{-4}$ )	Observed (ZV) ( $\text{TeV}^{-4}$ )	Expected (ZV) ( $\text{TeV}^{-4}$ )
$f_{S0}/\Lambda^4$	$[-4.2, 4.2]$	$[-40, 40]$	$[-31, 31]$
$f_{S1}/\Lambda^4$	$[-5.2, 5.2]$	$[-32, 32]$	$[-24, 24]$

- Other searches: Cut-Off used.

95% C.L. limits for  $\sqrt{s} = 13 \text{ TeV}, 35.9 \text{ fb}^{-1}$

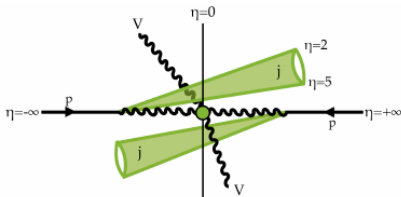
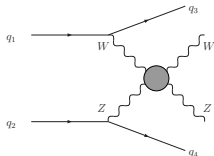
[Phys. Lett. B 798 (2019) 134985 (CMS)]

# Our computation of unitarity effects at $pp$ collisions

- 1.- Unitarization applied to **VBS** subprocess amplitude  $\Rightarrow \sigma(pp \rightarrow WZjj)$  computed with a Python code using the **Effective  $W$  Approximation**  
That is by means of a factorization connecting the subprocess with the process.
- 2.- Then we check the goodness of the **EWA** by comparing with full MG5  $pp \rightarrow WZjj$  events (**VBS**+others). Both in SM and EChL.
- 3.- We compare our predicted  $\sigma^{\text{EWA}}(pp \rightarrow WZjj)$  for a given unitarization method with LHC data in the  $(a_4, a_5)$  plane.
- 4.- **VBS** events usually selected by specific **VBS**-cuts: large pseudorapidity gap and large invariant mass (like  $\Delta\eta_{jj} > 4$  and  $M_{jj} > 500$  GeV).

$pp \rightarrow WZjj_1j_2$

by  $WZ \rightarrow WZ$  scattering

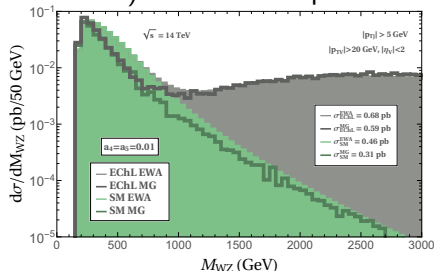


# Effective $W$ Approximation (EWA)

- $W$ 's and  $Z$ 's considered as partons inside the proton.  
Generalization of the Weizsäcker-Williams approximation for photons.
- They are emitted collinearly from the fermions (quarks) with probability functions  $f_V(\hat{x})$  and then scatter on-shell.
- Factorization using a sort of **PDFs**

$$\sigma(pp \rightarrow (V_1 V_2 \rightarrow V_3 V_4) + X) = \sum_{i,j} \int \int dx_1 dx_2 f_{q_i}(x_1) f_{q_j}(x_2) \int \int d\hat{x}_1 d\hat{x}_2 f_{V_1}(\hat{x}_1) f_{V_2}(\hat{x}_2) \hat{\sigma}(V_1 V_2 \rightarrow V_3 V_4)$$

- We have tested with MG5 the accuracy of various probability functions (SM and EChL): Dawson's Improved formulas work best!



[Nucl. Phys. B249 (1985) 42]

# More about the EWA

The most accurate EWA expression in our setup is the **Dawson's Improved**

$$f_{VT}^{Improved}(\hat{x}) = \frac{C_V^2 + C_A^2}{8\pi^2 \hat{x}} \eta \left[ \frac{-\hat{x}^2}{1 + M_V^2/(4E^2(1-\hat{x}))} + \frac{2\hat{x}^2(1-\hat{x})}{M_V^2/E^2 - \hat{x}^2} + \left\{ \hat{x}^2 + \frac{\hat{x}^4(1-\hat{x})}{(M_V^2/E^2 - \hat{x}^2)^2} \left( 2 + \frac{M_V^2}{E^2(1-\hat{x})} \right) \right. \right. \\ \left. \left. - \frac{\hat{x}^2}{(M_V^2/E^2 - \hat{x}^2)^2} \frac{M_V^4}{2E^4} \right\} \log \left( 1 + \frac{4E^2(1-\hat{x})}{M_V^2} \right) + \hat{x}^4 \left( \frac{2-\hat{x}}{M_V^2/E^2 - \hat{x}^2} \right)^2 \log \frac{\hat{x}}{2-\hat{x}} \right]$$

with  $C_{V(A)}$  the vector(axial) couplings  $Vq\bar{q}$ ,  $\hat{x}$  the fraction of

quark energy  $E = \frac{\sqrt{s_{q\bar{q}}}}{2}$  carried by  $V$  and  $\eta \equiv \left( 1 - \frac{M_V^2}{\hat{x}^2 E^2} \right)^{1/2}$

In the limit  $M_V \ll E$  (LLA)  $\Rightarrow$

$$f_{VT}^{LLA}(\hat{x}) = \frac{C_V^2 + C_A^2}{8\pi^2 \hat{x}} \left[ \hat{x}^2 + 2(1-\hat{x}) \right] \log \left( \frac{4E^2}{M_V^2} \right)$$

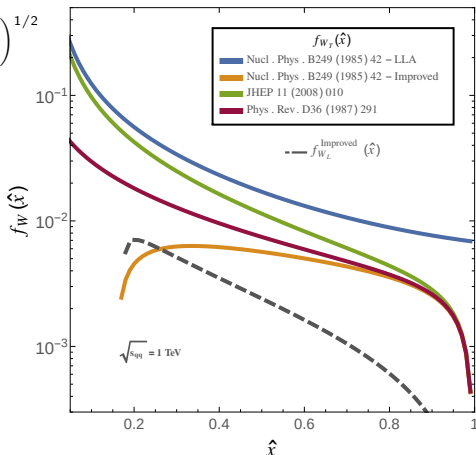
Among different  $f_V$

In the high  $\hat{x}$  region: similar results.

In the low  $\hat{x}$  region: differ quite a lot.

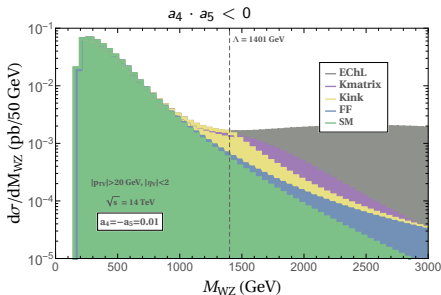
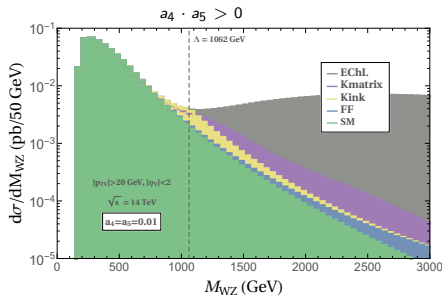
**Dawson's Improved** gets correct

$\sigma(pp \rightarrow WZ + jj)$  in low  $M_{WZ}$  region  
(most events here).



# Predictions with different unitarization methods at LHC

- Different results depending on unitarization method also at the LHC.
- Both distributions and cross sections result to be different.



Low  $M_{WZ}$  region: all procedures give very similar predictions (ChPT).

Non-unitarized EChL: SS  $a_4$  and  $a_5$  is more constrained than OS.

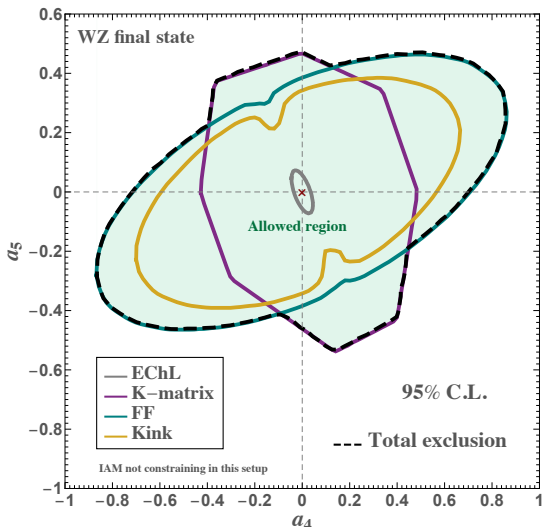
Form Factor and Kink: OS  $a_4$  and  $a_5$  is more constrained than SS.

Cut-Off scale is lower in the SS case.

In both SS and OS:  $\sigma_{\text{EChL}} > \sigma_{\text{K-matrix}} > \sigma_{\text{Kink}} > \sigma_{\text{FF}}$

# Our results: parameter uncertainty in $(a_4, a_5)$ plane

- We focus on  $WZ$  Run 1 ATLAS analysis ( $\sqrt{s} = 8$  TeV and  $\mathcal{L} = 20.2 \text{ fb}^{-1}$ )
- From the ATLAS 'ellipse' (contour at 95% C.L.) for  $K$ -matrix we extract our equivalent cross section.
- For the other unitarization methods, we construct the contours at 95% C.L.  
Main assumption: selection cuts affect equally all predictions.
- Non-unitarized gives strong constraints (small ellipse).  
 $a_4, a_5 > 0$  more constrained.
- Overlap corresponds to the uncertainty in  $(a_4, a_5)$
- Same game for linear EFTs.
- Shape and orientation change from one method to another.  
Size enhances by  $\sim 10$  the uncertainty respect to the non-unitarized constraints.



# Conclusions

- EFT is a powerful tool to study New Physics in a model-independent way.
- EChL is the most general EFT suitable for strongly interacting scenarios of EWSB. This EFT approach might lead to event predictions that violate unitarity.
- VBS is the key observable of this kind of physics.
- Unitarization methods must be applied in order to provide unitary predictions:
  - ⇒ different unitarization procedures lead to different predictions for VBS.
  - ⇒ a theoretical uncertainty is associated with this ambiguity.
- We provide a first approximation to quantify this uncertainty in the experimental determination of  $(a_4, a_5)$  due to the unitarization scheme choice through the elastic  $WZ$  scattering at the LHC.

⇒ this theoretical uncertainty can be large and it must be taken into account in the interpretation of the experimental data.

Thank you!



# Backup slides

# Transformations under $SU(2)_L \times SU(2)_R$

The rotations under  $SU(2)_L$  and  $SU(2)_R$  correspond to

$$g_L = e^{i\vec{\tau} \cdot \vec{\alpha}_L/2} \quad \text{and} \quad g_R = e^{i\vec{\tau} \cdot \vec{\alpha}_R/2}$$

Then building blocks transform under the global  $SU(2)_L \times SU(2)_R$  as

$$U \mapsto U' = g_L U g_R^\dagger \quad \text{with chiral dim.} = 0$$

$$\hat{B}_\mu \mapsto \hat{B}'_\mu = \hat{B}_\mu \quad \text{with chiral dim.} = 1$$

$$\hat{W}_\mu \mapsto \hat{W}'_\mu = g_L \hat{W}_\mu g_L^\dagger \quad \text{with chiral dim.} = 1$$

$$D_\mu U \mapsto (D_\mu U)' = g_L D_\mu U g_R^\dagger \quad \text{with chiral dim.} = 1$$

$$\hat{B}_{\mu\nu} \mapsto \hat{B}'_{\mu\nu} = \hat{B}_{\mu\nu} \quad \text{with chiral dim.} = 2$$

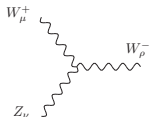
$$\hat{W}_{\mu\nu} \mapsto \hat{W}'_{\mu\nu} = g_L \hat{W}_{\mu\nu} g_L^\dagger \quad \text{with chiral dim.} = 2$$

For the EW gauge symmetry  $SU(2)_L \times U(1)_Y \subset SU(2)_L \times SU(2)_R$ , the association of the generator of  $U(1)_Y$  as the third one of the  $SU(2)_R$  and the generator of  $U(1)_{EM}$  as the third one of the  $SU(2)_{L+R}$ :

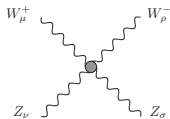
$$Y \leftrightarrow X_R^3 \quad \text{and} \quad Q \leftrightarrow X_{L+R}^3 = T^3 + Y$$

# Relevant Feynman rules for $A(WZ \rightarrow WZ)^{\text{EChL}}$

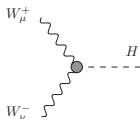
Simplified scenario: only effects of  $a$ ,  $a_4$  and  $a_5$



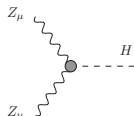
$$V_{W_\mu^+ W_\rho^- Z_\nu}^{\text{EChL}} = V_{W_\mu^+ W_\rho^- Z_\nu}^{\text{SM}}$$



$$V_{W_\mu^+ W_\rho^- Z_\nu Z_\sigma}^{\text{EChL}} = ig^2 c_w^2 \left[ g_{\mu\nu} g_{\rho\sigma} + g_{\mu\sigma} g_{\nu\rho} - 2g_{\mu\rho} g_{\nu\sigma} \right] + \frac{ig^4}{c_w^2} \left[ a_4 (g_{\mu\nu} g_{\rho\sigma} + g_{\mu\sigma} g_{\nu\rho}) + 2a_5 (g_{\mu\rho} g_{\nu\sigma}) \right]$$



$$V_{W_\mu^+ W_\nu^- H}^{\text{EChL}} = igM_W g_{\mu\nu} + igM_W (a-1) g_{\mu\nu}$$



$$V_{Z_\mu Z_\nu H}^{\text{EChL}} = \frac{igM_Z}{c_w} g_{\mu\nu} + \frac{igM_Z}{c_w} (a-1) g_{\mu\nu}$$

# Experimental searches for the ECHL parameters (95% C. L.)

- $a_1$ : EW precision measurements ( $S$  parameter) [Pyhs. Rev. D98 (2018) 030001 (PDG)]  
$$-0.12 < S^{obs} = -4\pi a_1 < 0.16$$
- $a_2$  and  $a_3$ : ATLAS global-fit in the search with  $\sqrt{s} = 13$  TeV and  $\mathcal{L} = 36$  fb $^{-1}$  looking for  $W^+W^-$  and  $W^\pm Z$  (full leptonic decays) via VBF  
[Pyhs. Rev. D99 (2019) 033001 (ATLAS)]  $\Rightarrow$  aTGC ( $\gamma W^+W^-$  and  $ZW^+W^-$ )  
$$-8.3 < \frac{f_B}{\Lambda^2} = \frac{8(a_2 - a_1)}{v^2} < 26 \text{ and } -3 < \frac{f_W}{\Lambda^2} = -\frac{8a_3}{v^2} < 3.7$$
- $a_4$  and  $a_5$ : CMS search for anomalous EW production of  $W^+W^-$ ,  $W^\pm Z$  and  $ZZ$  plus 2 jets with  $\sqrt{s} = 13$  TeV and  $\mathcal{L} = 36$  fb $^{-1}$   
[Phys. Lett. B 798 (2019) 134985 (CMS)]  $\Rightarrow$  aQGC ( $W^+W^-W^+W^-$  and  $ZZW^+W^-$ )  
$$-2.7 < \frac{f_{S0}}{\Lambda^4} = \frac{16a_4}{v^4} < 2.7 \text{ and } -3.4 < \frac{f_{S1}}{\Lambda^4} = -\frac{16a_5}{v^4} < 3.4$$
- $\Delta a$ : ATLAS combined measurements of all Higgs production and decay modes with  $\sqrt{s} = 13$  TeV and  $\mathcal{L} = 80$  fb $^{-1}$  [Phys. Rev. D101 012002 (ATLAS)]  
$$0.94 < \kappa_V = 1 + \Delta a < 1.14$$
- $\Delta b$ : ATLAS search for  $HH \rightarrow b\bar{b}b\bar{b}$  via VBF with  $\sqrt{s} = 13$  TeV and  $\mathcal{L} = 126$  fb $^{-1}$  [ATLAS-CONF-2019-030 (2001.05178)]  
$$-0.56 < \kappa_{2V} = 1 + \Delta b < 2.89$$

# Unitarized amplitudes

The partial wave decomposition is

$$a_{\lambda_1 \lambda_2 \lambda_3 \lambda_4}^J(s) = \frac{1}{32\pi} \int_{-1}^1 d\cos\theta A(V_{\lambda_1} V_{\lambda_2} \rightarrow V_{\lambda_3} V_{\lambda_4})(s, \cos\theta) d_{\lambda, \lambda'}^J(\cos\theta)$$

where  $J$  is the total angular momentum of the system,  $\lambda = \lambda_1 - \lambda_2$ ,  $\lambda' = \lambda_3 - \lambda_4$ , being  $\lambda_i$  the helicity states of the external gauge bosons, and where  $d_{\lambda, \lambda'}^J(\cos\theta)$  are the Wigner functions.

For the K-matrix and IAM methods, the unitarized amplitude is reconstructed from the corresponding unitarized partial wave and the non-unitary amplitudes following:

$$\begin{aligned} \hat{A}_{\lambda_1 \lambda_2 \lambda_3 \lambda_4}(s, \cos\theta) &= A_{\lambda_1 \lambda_2 \lambda_3 \lambda_4}(s, \cos\theta) \\ &\quad - 16\pi \sum_{J=0}^2 (2J+1) d_{\lambda, \lambda'}^J(\cos\theta) a_{\lambda_1 \lambda_2 \lambda_3 \lambda_4}^J(s) \\ &\quad + 16\pi \sum_{J=0}^2 (2J+1) d_{\lambda, \lambda'}^J(\cos\theta) \hat{a}_{[\lambda_1 \lambda_2 \lambda_3 \lambda_4]}^J(s) \end{aligned}$$

# More about the EWA

The most accurate EWA expression in our setup is the **Dawson's Improved**

$$f_{VT}^{Improved}(x) = \frac{C_V^2 + C_A^2}{8\pi^2 x} \left[ \frac{-x^2}{1 + M_V^2/(4E^2(1-x))} + \frac{2x^2(1-x)}{M_V^2/E^2 - x^2} + \left\{ x^2 + \frac{x^4(1-x)}{(M_V^2/E^2 - x^2)^2} \left( 2 + \frac{M_V^2}{E^2(1-x)} \right) \right. \right. \\ \left. \left. - \frac{x^2}{(M_V^2/E^2 - x^2)^2} \frac{M_V^4}{2E^4} \right\} \log \left( 1 + \frac{4E^2(1-x)}{M_V^2} \right) + x^4 \left( \frac{2-x}{M_V^2/E^2 - x^2} \right)^2 \log \frac{x}{2-x} \right] \eta$$

$$f_{VL}^{Improved}(x) = \frac{C_V^2 + C_A^2}{\pi^2} \frac{1-x}{x} \frac{\eta}{(1+\eta)^2} \left\{ \frac{1-x - M_V^2/(8E^2)}{1-x + M_V^2/(4E^2)} - \frac{M_V^2}{4E^2} \frac{1+2(1-x)^2}{1-x + M_V^2/(4E^2)} \frac{1}{M_V^2/E^2 - x^2} \right. \\ \left. - \frac{M_V^2}{4E^2} \frac{x^2}{2(1-x)(x^2 - M_V^2/E^2)^2} \left[ (2-x)^2 \log \frac{x}{2-x} - \left( \left( x - \frac{M_V^2}{E^2 x} \right)^2 - (2(1-x) + x^2) \right) \log \left( 1 + \frac{4E^2(1-x)}{M_V^2} \right) \right] \right. \\ \left. - \frac{M_V^2}{8E^2} \frac{x}{\sqrt{x^2 - M_V^2/E^2}} \left[ \frac{2}{x^2 - M_V^2/E^2} + \frac{1}{1-x} \right] \left[ \log \frac{2-x - \sqrt{x^2 - M_V^2/E^2}}{2-x + \sqrt{x^2 - M_V^2/E^2}} - \log \frac{x - \sqrt{x^2 - M_V^2/E^2}}{x + \sqrt{x^2 - M_V^2/E^2}} \right] \right\}$$

with  $C_{V(A)}$  the vector(axial) couplings  $Vq q$ ,  $x$  the fraction of

quark energy  $E = \frac{\sqrt{s} q q}{2}$  carried by  $V$  and  $\eta \equiv \left( 1 - \frac{M_V^2}{x^2 E^2} \right)^{1/2}$

In the limit  $M_V \ll E$  (LLA)  $\Rightarrow$

$$f_{VT}^{LLA}(x) = \frac{C_V^2 + C_A^2}{8\pi^2 x} \left[ x^2 + 2(1-x) \right] \log \left( \frac{4E^2}{M_V^2} \right)$$

$$f_{VL}^{LLA}(x) = \frac{C_V^2 + C_A^2}{\pi^2} \frac{1-x}{x}$$

